

Diffusion-MPC in Discrete Domains: Feasibility Constraints, Horizon Effects, and Critic Alignment: Case study with Tetris

Haochuan Kevin Wang
 Massachusetts Institute of Technology
 hcw@mit.edu

March 4, 2026

Abstract

We present DIFFTETRIS, a diffusion-style model predictive control (MPC) planner for Tetris that samples candidate placement sequences with a discrete denoiser and selects actions via reranking. We study three axes: (1) *feasibility-constrained sampling* via logit masking with valid placement masks; (2) *reranking* using a heuristic board score, a pretrained DQN critic, and a hybrid combination; and (3) *compute scaling* in the number of candidates. Our findings are fourfold. First, feasibility filtering is essential in this discrete domain: masking removes invalid action mass (mean masked fraction $\approx 46\%$) and yields a $6.8\times$ score gain and $5.6\times$ survival gain over unconstrained sampling. Second, naive DQN reranking is systematically misaligned with the rollout objective, producing large decision regret (mean 17.6, p90 36.6; regret > 10 in 63% of decisions at $H = 8$). Third, shorter horizons can outperform longer ones (heuristic $H = 4$: 1.48 score, 1663ms; $H = 8$: 0.89 score, 2761ms), consistent with sparse/delayed rewards and uncertainty compounding in longer imagined rollouts. Fourth, compute choices (K, H) shape the dominant failure mode: small K limits candidate quality, while larger H amplifies mismatch and misranking.

1 Introduction

Diffusion models have emerged as powerful generative models across images, video, and most recently, sequential decision-making [Ho et al., 2020, Janner et al., 2022, Ajay et al., 2023]. In the planning setting, a diffusion model generates candidate action trajectories conditioned on the current state, and the best trajectory is selected for execution—a paradigm known as diffusion-MPC [Janner et al., 2022, Liang et al., 2024].

A key challenge in applying diffusion planners to discrete, combinatorial domains is ensuring that sampled trajectories respect environment constraints. Unlike continuous control where small deviations may be tolerable, discrete action spaces with hard validity constraints—such as piece placement legality in Tetris—mean that a single infeasible action renders an entire candidate trajectory unusable.

We study this problem in the domain of Tetris, a canonical combinatorial puzzle known to be NP-hard even to approximate [Demaine et al., 2003]. Tetris provides an ideal testbed: the action space is discrete (rotation \times x-position), validity constraints are piece-dependent and board-state-dependent, and episodes are long enough to expose compounding errors.

Our contributions are as follows. First, we implement and evaluate a MaskGIT-style [Chang et al., 2022] discrete diffusion planner for Tetris, where a conditional Transformer denoiser generates candidate $(rotation, x)$ token sequences. Second, we demonstrate that *feasibility-constrained sampling*—masking logits against valid placement masks at each autoregressive step—is necessary for performance, improving mean score from 0.13 to 0.89 and survival rate from 5% to 28% by restoring a valid search space. Third, we show that replacing the heuristic reranking function with a learned DQN critic [Mnih et al., 2015] *harms* performance despite the critic being trained on the same domain, and we diagnose this failure using *decision-level regret*: the gap between the rollout score of the chosen candidate and the best available candidate. Finally, we characterize how compute choices (K, H) change failure modes: increasing K strongly improves quality at fixed H , whereas increasing horizon can degrade both quality and latency; a hybrid reranking approach recovers heuristic-level performance while limiting critic harm.

2 Background and Related Work

Diffusion models for planning. Diffuser [Janner et al., 2022] introduced diffusion models as trajectory generators for offline reinforcement learning, sampling full state-action trajectories and using classifier guidance or reward-weighted sampling for optimization. Decision Diffuser [Ajay et al., 2023] showed that conditional generation can subsume many decision-making paradigms. AdaptDiffuser [Liang et al., 2023] extended this with self-evolving adaptation. Diffusion Policy [Chi et al., 2023] applied diffusion-based action generation to visuomotor control. These works primarily operate in continuous state-action spaces; our work extends diffusion planning to *discrete* combinatorial domains with hard feasibility constraints.

Model predictive control with sampling. Sampling-based MPC generates candidate action sequences from a proposal distribution and selects the best according to a scoring function [Williams et al., 2017, Nagabandi et al., 2018]. Our approach follows this paradigm, using a trained diffusion model as the proposal distribution and evaluating candidates via forward simulation.

Masked generative models. MaskGIT [Chang et al., 2022] introduced iterative parallel decoding for discrete token generation, where tokens are progressively unmasked based on confidence. Our PlanDenoiser adopts this architecture for action sequence generation, with the critical addition of feasibility masking at sampling time.

Deep Q-Networks. DQN [Mnih et al., 2015] learns state-action value functions from environment interaction. We use a pre-trained DQN as a candidate reranking critic, evaluating whether learned value estimates can improve upon heuristic scoring in the MPC selection step.

3 Method

3.1 Problem Setup

We consider Tetris on a 20×10 board. At each decision step, the agent observes the current board state $b \in \{0, 1\}^{20 \times 10}$, the current piece identity $c \in \{0, \dots, 6\}$, and the next piece identity $n \in \{0, \dots, 6\}$. The action space is the set of placements (r, x) where $r \in \{0, 1, 2, 3\}$ is the rotation index and $x \in \{0, \dots, 9\}$ is the horizontal position, yielding $|\mathcal{A}| = 40$ discrete actions. Not all actions are valid for a given (b, c) pair; the set of valid actions $\mathcal{V}(b, c) \subseteq \mathcal{A}$ depends on the piece geometry and board configuration.

Diffusion-MPC Planning Step

```
Input: State  $(b, c, n)$ , denoiser  $f_\theta$ , candidates  $K$ , horizon  $H$ 
for  $k = 1, \dots, K$  do
  1. Sample  $s_k = \{(r_h, x_h)\}_{h=1}^H$  from  $f_\theta$ 
  2. Simulate  $s_k$  in cloned environment
  3. Compute reranking score  $v_k$ 
end for
 $k^* \leftarrow \arg \max_k v_k$ 
return first action of  $s_{k^*}$ 
```

Figure 1: Pseudocode for the diffusion-MPC planning step.

3.2 PlanDenoiser Architecture

The core generative model is a conditional Transformer [Vaswani et al., 2017] that we call PlanDenoiser. It takes as input the board state (encoded via a 2-layer CNN), piece embeddings for c and n , and a sequence of partially-masked (r, x) token pairs of length H (the planning horizon). The model outputs logits over rotation ($\mathbb{R}^{B \times H \times 4}$) and x-position ($\mathbb{R}^{B \times H \times W}$).

Specifically, the board is encoded as $\text{CNN}(b) \in \mathbb{R}^{d_{\text{feat}}}$, concatenated with learned piece embeddings $e_c, e_n \in \mathbb{R}^{16}$, and projected to the model dimension $d = 128$. This condition vector serves as the first token in a sequence of $H + 1$ tokens. The remaining H tokens are the sum of rotation and x-position embeddings. A learned positional embedding is added, and the sequence is processed by a 4-layer Transformer encoder with 4 attention heads.

Training. The model is trained with a MaskGIT-style [Chang et al., 2022] masked prediction objective. During training, a random fraction of the H token positions are replaced with mask tokens, and the model is trained to predict the original tokens at masked positions via cross-entropy loss. Training data consists of expert trajectories generated by a heuristic Tetris agent.

3.3 MPC Planning Loop

At evaluation time, we use the trained PlanDenoiser within a sampling-based MPC framework (Algorithm 1). Given the current state (b, c, n) , we sample K candidate action sequences of length H from the denoiser, score each candidate by forward simulation, and execute the first action of the highest-scoring candidate.

3.4 Feasibility-Constrained Sampling

In the unconstrained setting (sampling_constraints=none), the denoiser uses the standard MaskGIT iterative refinement procedure: all K candidates are sampled in parallel

using S denoising steps, progressively locking in the most confident tokens.

In the feasibility-constrained setting (sampling constraints = mask_logits), we modify the sampling to be autoregressive over the horizon. At each horizon step h , we compute the valid placement mask $m \in \{0, 1\}^{4W}$ for the current simulated board state using valid_placement_mask, which enumerates all (r, x) pairs and checks geometric feasibility. We form joint logits over the flattened action space as $\ell_{r,x} = \ell_r^{(\text{rot})} + \ell_x^{(\text{pos})}$ and mask invalid entries: $\ell_{r,x} \leftarrow -\infty$ where $m_{rW+x} = 0$. Sampling from the resulting softmax distribution guarantees that every sampled action is feasible.

This masking incurs a computational cost: candidates must be sampled sequentially rather than in parallel, since each step requires simulating the previous action to obtain the updated board state for masking. In our experiments, approximately 46% of the action space is masked on average, indicating that nearly half of all placements are infeasible at any given step.

3.5 Reranking Strategies

After sampling K candidates, we must select which candidate to execute. We study three reranking strategies:

Heuristic reranking. Each candidate is scored by simulating its action sequence in a cloned environment and evaluating the resulting board state with a hand-crafted heuristic: $v = 5.0 \cdot \text{lines} - 0.8 \cdot \text{holes} - 0.05 \cdot \text{height} - 0.03 \cdot \text{bump} - 0.02 \cdot \text{max_h}$. This heuristic captures well-known properties of good Tetris play.

DQN reranking. We replace the heuristic scorer with a pre-trained DQN critic [Mnih et al., 2015]. The DQN is a CNN-based Q-network trained via standard deep Q-learning on the same Tetris environment. The value of a candidate is $V(b') = \max_{a \in \mathcal{V}(b', c')} Q(b', c', n'; a)$, where b' is the board state after simulating the candidate.

Hybrid reranking. We combine both signals: $v_k^{\text{hybrid}} = v_k^{\text{rollout}} + \alpha \cdot z(v_k^{\text{dqn}})$, where v_k^{rollout} is the heuristic rollout score, $z(\cdot)$ denotes z-score normalization across the K candidates, and α is a mixing weight. The z-scoring ensures the DQN contribution is scale-invariant.

3.6 Decision-Level Regret

We introduce *decision-level regret* as a diagnostic for reranking quality. For each decision step, we compute the heuristic rollout score of every candidate and define regret as:

$$\text{regret}_t = \max_k v_k^{\text{rollout}} - v_{k^*}^{\text{rollout}}, \quad (1)$$

where k^* is the candidate selected by the reranking strategy. When the reranking criterion aligns with the rollout score (as in heuristic reranking), regret is identically zero. When a misaligned critic selects a different candidate, regret measures the opportunity cost.

4 Experimental Setup

Environment. We use a custom Tetris implementation with a 20×10 board, 7 standard tetrominoes, and placement-based actions. Each episode runs until game over or a maximum of 2000 steps. All evaluations use 100 episodes with a fixed random seed for reproducibility.

PlanDenoiser training. The denoiser is trained on expert trajectories from a heuristic agent using the “loose” dataset variant. The model uses $d = 128$, 4 Transformer layers, 4 heads, and is trained with a MaskGIT masked prediction objective on sequences of horizon $H = 8$. The denoising process uses $S = 8$ iterative refinement steps at temperature $\tau = 1.0$.

DQN critic. The DQN is a CNN-based Q-network with separate current-piece and next-piece embeddings, trained via standard DQN with experience replay on the same Tetris environment.

Horizon mismatch handling. When evaluating with a horizon $H_{\text{eval}} < H_{\text{train}}$, the learned positional embedding is truncated to the first $H_{\text{eval}} + 1$ positions. This allows a single checkpoint trained at $H = 8$ to be evaluated at $H = 4$ without retraining.

Configurations. We evaluate the following configurations:

- **Baseline:** No masking + heuristic reranking ($K = 64, H = 8$)
- **Mask + Heuristic:** Feasibility masking + heuristic ($K = 64, H = 8$)
- **Mask + DQN:** Feasibility masking + DQN reranking ($K = 64, H \in \{4, 8\}$)
- **Mask + Hybrid:** Feasibility masking + hybrid with $\alpha = 0.05$ ($K = 64, H = 8$)
- **Scaling:** Mask + heuristic with $K \in \{16, 32, 64\}$ ($H = 8$)

5 Results

5.1 Main Results

Table 1 presents the full results across all configurations.

Table 1: Main evaluation results across configurations (100 episodes each). Regret measures the gap between chosen and best candidate rollout scores. All runs use $S = 8$ denoising steps and $\tau = 1.0$.

Configuration	Constraint	Rerank	H	K	Mean	Med.	Steps	%>0	ms/dec	Mask%	Regret (mean / p90)
No Mask + Heur	none	heuristic	8	64	0.13	0.0	16.0	5%	521	0.0%	0.00 / 0.0
Mask + Heur	mask	heuristic	8	64	0.89	0.0	25.9	28%	2761	46.3%	0.00 / 0.0
Mask + Heur ($K=16$)	mask	heuristic	8	16	0.31	0.0	24.4	12%	677	47.5%	0.00 / 0.0
Mask + Heur ($K=32$)	mask	heuristic	8	32	0.44	0.0	25.1	16%	1364	47.3%	0.00 / 0.0
Mask + Heur ($H=4$)	mask	heuristic	4	64	1.48	0.0	27.3	38%	1663	45.2%	0.00 / 0.0
Mask + DQN ($H=8$)	mask	dqn	8	64	0.14	0.0	23.5	7%	2492	48.5%	17.59 / 36.6
Mask + DQN ($H=4$)	mask	dqn	4	64	0.14	0.0	22.8	7%	1564	46.8%	11.47 / 24.6
Mask + Hybrid	mask	hybrid	8	64	0.89	0.0	25.5	29%	2832	46.2%	0.00 / 0.0

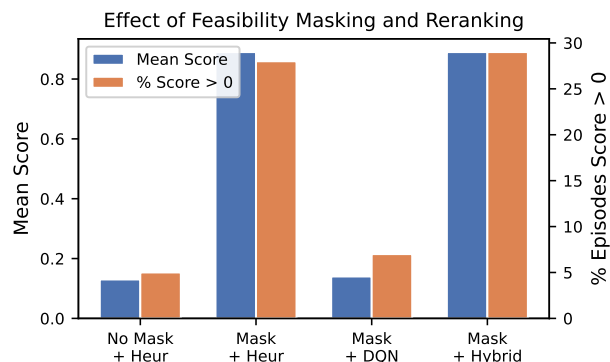


Figure 2: Effect of feasibility masking and reranking strategy on mean episode score and percentage of episodes achieving score > 0 . Masking yields a $6.8\times$ improvement. DQN reranking erases the masking benefit.

5.2 Effect of Feasibility Masking

Figure 2 shows the impact of feasibility-constrained sampling. Without masking, the baseline achieves a mean score of only 0.13 with 5% of episodes scoring above zero, surviving an average of 16 steps before termination. With masking enabled (and the same heuristic reranking), mean score increases to 0.89 ($6.8\times$), survival rate to 28% ($5.6\times$), and mean steps to 25.9 ($1.6\times$).

The masked fraction of approximately 46% confirms that nearly half of all candidate placements are geometrically infeasible at any given step. This indicates that masking is not merely a small regularizer; it changes the planner from sampling many non-executable actions to searching within feasible trajectories. Using episode length as a proxy for failure-to-act, 91% of unmasked episodes terminate within 20 steps versus 23% with masked heuristic sampling at $H = 8$. Thus, the primary gain from masking is restoring effective candidate diversity in the executable action space.

5.3 Compute-Quality Frontier and Critic Alignment

Figure 3 summarizes the quality-latency tradeoff across all evaluated configurations. The shortest-horizon masked heuristic configuration ($H = 4$) lies on the Pareto frontier and dominates the standard $H = 8$ setup, achieving both higher score (1.48 vs. 0.89) and lower latency (1663ms vs. 2761ms). This suggests that in this domain, longer lookahead can be counterproductive when rollout uncertainty compounds over horizon.

Replacing the heuristic reranker with the DQN critic dramatically degrades performance at both horizons: mean score drops to 0.14 and survival to 7%. In contrast, the hybrid reranker remains close to heuristic performance at $H = 8$ (0.89 score, 29% survival), indicating that bounded critic influence is safer than pure critic selection. Decision-level regret makes the failure mode explicit: DQN reranking has high regret (mean 17.59 at $H = 8$, 11.47 at $H = 4$), regret > 10 in 63.1% ($H = 8$) and 48.3% ($H = 4$) of decisions, whereas heuristic and hybrid reranking stay near zero. Because regret is defined as the gap to the best available candidate under the same rollout evaluator, positive regret directly certifies anti-helpful selections relative to that objective. Regret is highest early in episodes (mean 30.3 in the first quartile of steps for DQN $H = 8$, versus 5.7 in the last quartile), indicating that critic misranking occurs before deep-horizon compounding dominates.

This indicates a fundamental misalignment between the DQN’s value estimates and actual board quality as measured by forward simulation. The DQN may have learned a value function that is accurate in expectation over its own policy but misleading when used to evaluate trajectories generated by a different proposal distribution.

5.4 Hybrid Reranking

The hybrid strategy with $\alpha = 0.05$ recovers the full performance of heuristic reranking (mean score 0.89, survival 29%) while maintaining near-zero regret (mean 4.2×10^{-4} , p90 = 0.0). The small α ensures that the DQN signal acts only as a tiebreaker when rollout scores are close, preventing the critic from overriding clearly better candi-

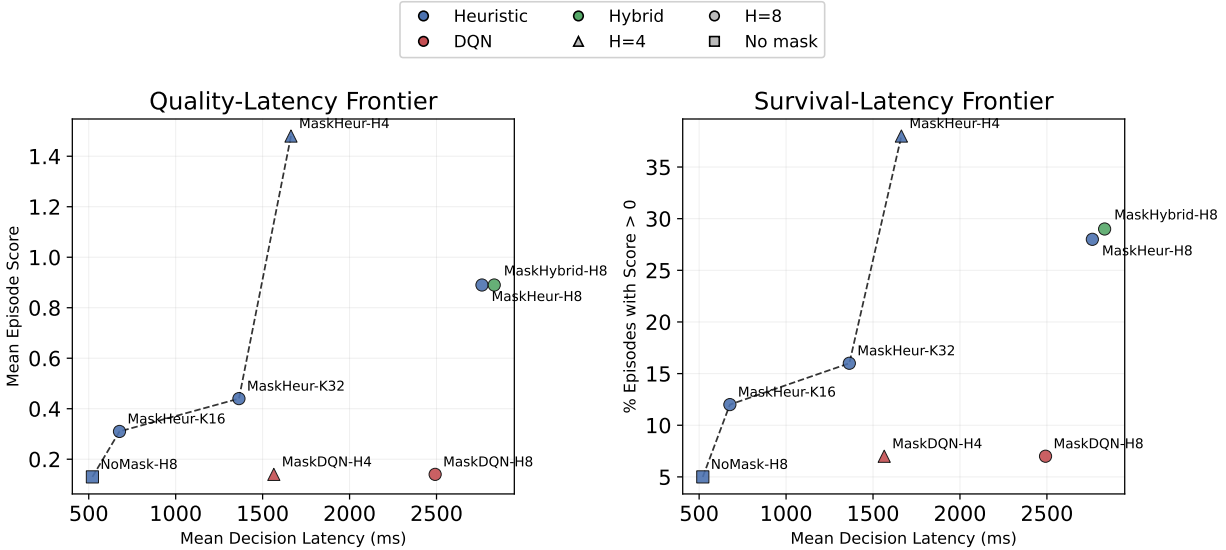


Figure 3: Compute-aware frontier across configurations. **Left:** mean score vs. decision latency. **Right:** survival rate (% episodes with score > 0) vs. latency. Dashed lines show Pareto frontiers. The masked heuristic $H = 4$ configuration is both faster and stronger than masked $H = 8$, while DQN reranking is off-frontier at both horizons.

dates. This demonstrates that learned critics can be safely integrated into sampling-based planners when their influence is appropriately bounded.

5.5 Compute Scaling

Figure 4 shows mean score as a function of the number of candidates K with masking and heuristic reranking at $H = 8$. Performance scales monotonically: $K = 16$ achieves 0.31, $K = 32$ achieves 0.44, and $K = 64$ achieves 0.89. This strongly increasing trend suggests that proposal quality is compute-limited in this regime: larger K increases the chance of sampling high-quality trajectories from the same denoiser. However, wall-clock time scales linearly with K (from 677ms to 2761ms per decision), presenting a clear compute-performance tradeoff. Latency-normalized score (1000-mean score/ms per decision) peaks at $K = 16$ (0.458) while raw score peaks at $K = 64$ (0.89), showing that deployment objectives (throughput vs. absolute quality) select different operating points.

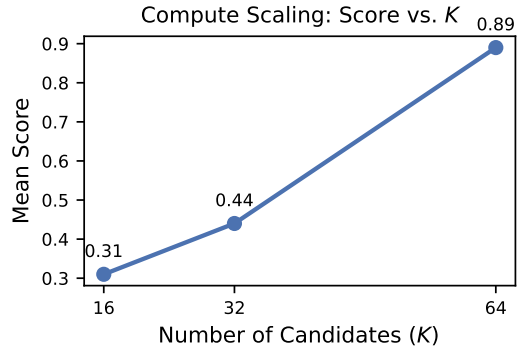


Figure 4: Compute scaling: mean episode score vs. number of candidates K , with feasibility masking and heuristic reranking ($H = 8$). Performance increases strongly with K , while latency grows approximately linearly.

5.6 Horizon Effects

An unexpected finding is that the shorter horizon $H = 4$ with heuristic reranking (mean score 1.48, survival 38%) *outperforms* $H = 8$ (mean score 0.89, survival 28%). This is consistent with sparse/delayed reward structure and objective mismatch: the denoiser is behavior-cloned on short-horizon targets, while planning quality depends on long-term return. With $H = 8$, a larger fraction of each candidate trajectory relies on imagined futures (unknown

piece sequences beyond the next piece), increasing distribution shift in simulated states and making late-token completions less reliable. The $H = 4$ configuration also benefits from lower computational cost per candidate (1663ms vs. 2761ms), since fewer autoregressive steps require fewer environment simulations for masking. Under DQN reranking, shortening horizon also reduces misranking severity (mean regret 17.59 \rightarrow 11.47; p90 36.6 \rightarrow 24.6), further supporting the view that longer-horizon rollouts amplify critic-planner mismatch.

6 Discussion and Limitations

Regret as a diagnostic. Our decision-level regret metric provides a model-free diagnostic for critic quality in sampling-based planners. When regret is consistently zero (as under heuristic reranking), the selection criterion is aligned with trajectory quality. When regret is large (as under DQN reranking), the critic is systematically misidentifying good candidates. Since regret is computed against the best available candidate at each decision, it is a direct per-step certificate of anti-helpful critic behavior under the rollout objective. This diagnostic does not require ground-truth value functions and can be computed online during evaluation.

Why does DQN reranking fail? We hypothesize several contributing factors. First, the DQN was trained under its own behavioral distribution, which differs from the diffusion planner’s proposal distribution; Q-values may not transfer to out-of-distribution states encountered during rollouts. Second, the DQN evaluates single-step state quality, while the rollout heuristic evaluates multi-step outcomes—these objectives may conflict. Third, the heuristic explicitly penalizes holes and bumpiness, which are strong predictors of near-term survival in Tetris; the DQN may have learned a smoother but less locally-accurate value function. Fourth, this mismatch worsens with horizon as rollouts move deeper into imagined futures, which increases critic OOD exposure.

Compute-dependent failure modes. Our sweeps suggest two distinct regimes. At low candidate count K , quality is dominated by proposal scarcity: increasing K substantially improves outcomes. At larger horizon H , quality is dominated by alignment and uncertainty: critic misranking and long-horizon simulation error become the limiting factors even when K is fixed. Thus, (K, H) tuning is not only a speed-accuracy tradeoff; it determines which failure mechanism dominates.

Limitations. Our study has several limitations. First, absolute performance remains modest (mean score < 2), reflecting the difficulty of Tetris and limited denoiser capacity/data. Second, rewards are sparse and delayed, while our denoiser is trained by behavior cloning rather than return optimization; this may inherently favor short-horizon proxy quality over long-horizon return. Third, our regret metric is defined relative to heuristic rollout score, which is a consistent internal objective but not true environment return. Fourth, feasibility-constrained masking requires sequential simulation to compute validity masks, reducing parallelism and increasing inference cost. Fifth, we evaluate on a single domain with 100 episodes per con-

figuration; broader generalization and tighter uncertainty estimates remain open.

Future work. Several directions are promising. Scaling the denoiser capacity and training data could improve base plan quality. Adaptive α scheduling for hybrid reranking could dynamically balance heuristic and critic signals. Constrained parallel sampling methods could recover the efficiency of batch generation while maintaining feasibility. Finally, training the denoiser with a planning-aware objective (e.g., decision-time fine-tuning) rather than pure behavior cloning could better align the proposal distribution with high-quality plans.

7 Conclusion

We presented DIFFTETRIS, a diffusion-style MPC planner for Tetris that combines a MaskGIT-based discrete denoiser with feasibility-constrained sampling and candidate reranking. Our results show that diffusion-MPC performance in discrete sparse-reward planning hinges less on generative modeling alone than on feasibility filtering, critic alignment, and compute choices. Feasibility-constrained masking converts a large invalid action mass ($\approx 46\%$) into executable candidates and delivers large gains in score and survival. Naive DQN reranking is not merely noisy but systematically anti-helpful under the rollout objective, with large decision regret and frequent severe misranking. Shorter horizon can dominate longer horizon on both quality and latency, consistent with uncertainty compounding through imagined futures and behavior-cloned short-term priors rather than direct long-term return optimization. Finally, (K, H) tuning changes which failure mode dominates: proposal scarcity at low K versus alignment and rollout uncertainty at larger H . These findings suggest that diffusion-MPC for combinatorial control should prioritize feasibility-aware sampling, regret-based alignment diagnostics, and compute-aware operating-point selection; learned critics likely require explicit distributional alignment or return-aware training objectives before they can be safely trusted for reranking.

Acknowledgements

We used the Tetris codebase from github.com/WilliamPig/tetris_ai to set up the Tetris playing ground used in this work.

References

Anurag Ajay, Yilun Du, Abhi Gupta, Joshua B Tenenbaum, Tommi Jaakkola, and Pukit Agrawal. Is conditional generation all you need for decision-making? In

- International Conference on Learning Representations*, 2023.
- Huiwen Chang, Han Zhang, Lu Jiang, Ce Liu, and William T Freeman. MaskGIT: Masked generative image transformer. In *Proceedings of the IEEE/CVF Conference on Computer Vision and Pattern Recognition*, pages 11315–11325, 2022.
- Cheng Chi, Siyuan Feng, Yilun Du, Zhenjia Xu, Eric Cousineau, Benjamin Burchfiel, and Shuran Song. Diffusion policy: Visuomotor policy learning via action diffusion. In *Robotics: Science and Systems*, 2023.
- Erik D Demaine, Susan Hohenberger, and David Liben-Nowell. Tetris is hard, even to approximate. *International Journal of Computational Geometry & Applications*, 13(06):495–519, 2003.
- Jonathan Ho, Ajay Jain, and Pieter Abbeel. Denoising diffusion probabilistic models. In *Advances in Neural Information Processing Systems*, volume 33, pages 6840–6851, 2020.
- Michael Janner, Yilun Du, Joshua B Tenenbaum, and Sergey Levine. Planning with diffusion for flexible behavior synthesis. In *International Conference on Machine Learning*, pages 9902–9915. PMLR, 2022.
- Guangyao Liang, Nishit Patel, Michael Luo, Zixuan Zhang, Debadeepta Dey, and Azalia Mirhoseini. Diffusion model predictive control. In *arXiv preprint arXiv:2408.09349*, 2024.
- Zhixuan Liang, Yao Mu, Mingyu Ding, Fei Ni, Masayoshi Tomizuka, and Ping Luo. AdaptDiffuser: Diffusion models as adaptive self-evolving planners. In *International Conference on Machine Learning*, pages 20725–20745. PMLR, 2023.
- Volodymyr Mnih, Koray Kavukcuoglu, David Silver, Andrei A Rusu, Joel Veness, Marc G Bellemare, Alex Graves, Martin Riedmiller, Andreas K Fidjeland, Georg Ostrovski, et al. Human-level control through deep reinforcement learning. *Nature*, 518(7540):529–533, 2015.
- Anusha Nagabandi, Gregory Kahn, Ronald S Fearing, and Sergey Levine. Neural network dynamics for model-based deep reinforcement learning with model-free fine-tuning. In *IEEE International Conference on Robotics and Automation*, pages 7559–7566, 2018.
- Ashish Vaswani, Noam Shazeer, Niki Parmar, Jakob Uszkoreit, Llion Jones, Aidan N Gomez, Łukasz Kaiser, and Illia Polosukhin. Attention is all you need. In *Advances in Neural Information Processing Systems*, volume 30, 2017.
- Grady Williams, Nolan Wagener, Brian Goldfain, Paul Drews, James M Rehg, Byron Boots, and Evangelos A Theodorou. Information theoretic MPC for model-based reinforcement learning. *IEEE International Conference on Robotics and Automation*, pages 1714–1721, 2017.